Interior responses to impacts by different impactor types

Thomas Ruedas[1,2,*], Doris Breuer[2]

[1]*Institute of Planetology, Westfälische Wilhelms-Universität Münster, Germany*
[2]*Institute of Planetary Research, German Aerospace Center (DLR), Berlin*

[*]Corresponding author email: t.ruedas@uni-muenster.de

Motivation

Several numerical mantle convection studies have investigated the effects of very large meteorite impacts on mantle dynamics in terrestrial planets, especially Mars (e.g., Watters *et al.*, 2009; Roberts and Arkani-Hamed, 2012). The impactors were generally assumed to have material parameters similar to those of the target. However, there is a significant fraction of potential impactors whose properties differ substantially from those of the target, and the dynamical effects in the interior may be quite different even if the final crater is similar; candidate alternative impactors include C-type asteroids and comets. It is generally not possible to deduce the nature of the impactor from the final crater, because the remnants of the impactor are rarely preserved. We show by analysing scaling laws how different impactors may result in the same final crater on a given planet. Some dynamical effects for different impactor types for Mars are then investigated with 2-D numerical mantle convection simulations using a modified version of STAGYY (Tackley, 2008; Ruedas *et al.*, 2013) in which the impact is represented as an instantaneous thermal anomaly. The models show that the effects on the interior of "isocrater" impacts by impactors of different types can vary considerably, especially between rocky impactors with low to intermediate velocities and fast, ice-rich impactors.

Model properties

The present models are not designed to be approximations of the real planet Mars, but they do use the characteristics of two major martian impacts (Utopia, Hematite) on a somewhat Mars-like body.

Convection model parameters: Initial potential temperature: 1700 K; initial T step across CMB: 150 K; 15fold viscosity increase between upper and lower half of mantle; radionuclide concentrations from Wänke and Dreibus (1994), Mg#=0.75, 36 wppm water; melting included, threshold for melt extraction: 0.7%; large (R_c = 1730 km) liquid iron–sulfur (16 wt.% S) alloy core, no basal bridgmanite+ferropericlase layer in the mantle; duration: 4.4 Gy

Impacts: All impactors strike at 4 Ga at an angle of 45°.
Impactor types: S-type asteroid: 2700 kg/m^3, 9.6 km/s; C-type asteroid: 1330 kg/m^3, 9.6 km/s; long-period comet (LPC): 540 kg/m^3, 45 km/s; TNO-type body: 1060 kg/m^3, 24.01 km/s (impact velocities for Mars)
Utopia-sized (final crater diameter: 3380 km, impactor diameter: 699 km), Hematite-sized (final crater diameter: 1065 km, impactor diameter: 187 km)

Theory

The diameters of the final crater, D_f, and of the impactor D_imp are related by

$$D_\mathrm{f} = 1.3836\left(\frac{\varrho_\mathrm{imp}}{\varrho}\right)^{0.377}\frac{D_\mathrm{imp}^{0.88}v_\mathrm{imp}^{0.497}}{D_\mathrm{s2c}^{0.13}g^{0.249}} \quad (1)$$

for complex craters, where ϱ and ϱ_imp are the densities of the target and the impactor, v_imp is the vertical component of the velocity of the impactor, D_s2c is the simple-to-complex transition diameter, and g is gravity (e.g., Werner and Ivanov, 2015); the numerical values of the coefficient and exponents vary with certain target properties and are chosen here to correspond to a frictionless, pore-free material. In this equation, ϱ_imp and v_imp are not known for a given crater and may vary widely between different impactor types. Hence the condition for two impactors 1 and 2 to produce a final crater of the same diameter on the same target is given by $D_\mathrm{f1} = D_\mathrm{f2}$:

$$\frac{D_\mathrm{imp1}}{D_\mathrm{imp2}} = \left(\frac{\varrho_\mathrm{imp1}}{\varrho_\mathrm{imp2}}\right)^{-0.43}\left(\frac{v_\mathrm{imp1}}{v_\mathrm{imp2}}\right)^{-0.56} = \delta_{12}, \quad (2)$$

for both simple and complex craters; this defines a set of isocrater impacts. Figure 1a shows the ratio of impactor diameters, δ_{12}, for isocrater impacts, whereby impactor 2 is chosen as a common reference impactor (S-type asteroid). The isolines thus show how strongly the size of impactor 1 must differ from that reference in order to produce a crater of the same size, for any combination of density and velocity, which are also normalized to the reference.

For the dynamics of the interior, it is rather the subsurface features of an impact that are of primary interest, but they are less well described in terms of an analytical model. The depth of penetration is often found to be proportional to $\sqrt{\varrho_\mathrm{imp}/\varrho}$. We combine this relation with the widely used formula by Pierazzo *et al.* (1997) for the depth to the center of the isobaric core of the shocked volume:

$$z_\mathrm{ic} = 0.1524 D_\mathrm{imp} v_\mathrm{imp}^{0.361}\sqrt{\frac{\varrho_\mathrm{imp}}{\varrho}}. \quad (3)$$

The ratio of the depths of the isobaric cores for two isocrater impacts then follows from eq. 2:

$$\frac{z_\mathrm{ic1}}{z_\mathrm{ic2}} = \left(\frac{\varrho_\mathrm{imp1}}{\varrho_\mathrm{imp2}}\right)^{0.07}\left(\frac{v_\mathrm{imp1}}{v_\mathrm{imp2}}\right)^{-0.199} = \zeta_{12} \quad (4)$$

(cf. Figure 1b). An analogous relation can be derived for the shocked volume (see abstract).

There are also semi-empirical relations between impactor parameters and the amount of melt produced in an impact. Combining a scaling law originally by Bjorkman and Holsapple (1987), we have

$$\lambda_{12} = \frac{V_\mathrm{m1}}{V_\mathrm{m2}} = \left(\frac{\varrho_\mathrm{imp1}}{\varrho_\mathrm{imp2}}\right)^{\nu-1.29}\left(\frac{v_\mathrm{imp1}}{v_\mathrm{imp2}}\right)^{3\mu-1.68}, \quad (5)$$

where V_m is the melt volume and ν and $\mu = 0.47\ldots0.58$ are constants related to the target. We set $\nu = 1$ (Abramov *et al.*, 2012). – In the numerical models, we calculate melting directly from the thermal anomaly and its dynamics, however.

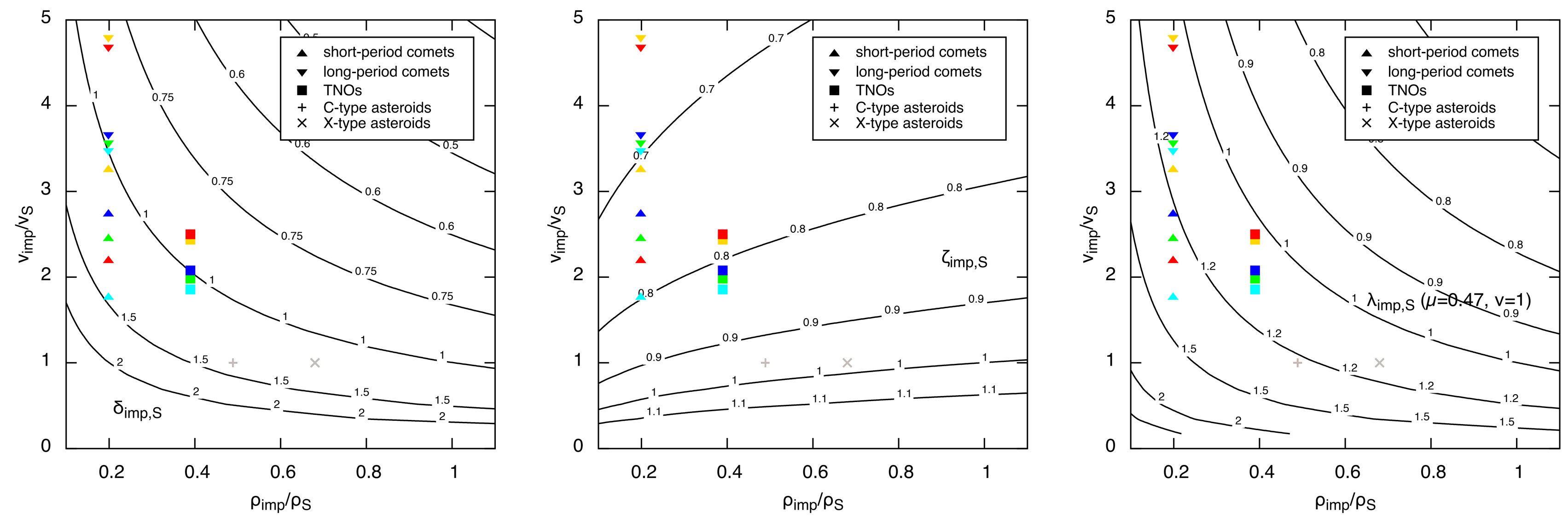

Fig. 1: Ratios of impactor diameters (left), depth to the center of the isobaric core (center), and melt production (right) for impacts resulting in final craters of the same size as functions of the ratios of densities and impactor velocities according to eqs. 2, 4, and 5; the reference impactor for the ratios is an S-type asteroid. The symbols mark average values pertaining to the target planet (cyan: Mercury, green: Venus, blue: Earth, gold: Moon, red: Mars, grey: all target bodies), their shapes indicate the impactor type. S-, C-, and X-type asteroids are assumed to have the same average velocities at a given target.

All plots in Fig. 1 apply to impacts of impactors that differ in density, velocity, and size but result in a crater of the same final diameter. The dots correspond to mean values for the impactor densities and velocities at each target. The isolines in Fig. 1a show how much larger or smaller, relative to an S-type asteroid, an impactor of some chosen density and velocity has to be in order to produce the same crater; e.g., a C-type asteroid, which is about half as dense as an S-type asteroid but has the same velocity, would have to a have 1.4 times the diameter, regardless of the target, whereas a TNO-like impactor, which is even less dense but considerably faster, would have to be about 15% smaller on Mars or the Moon but almost the same size on Earth, Venus, or Mercury. Fig. 1b shows that the center of the isobaric core would be shallower for all alternative impactor types, although only slightly so for asteroid impactors. On the other hand, V_m for alternative impactors would be larger by up to 40%, depending on impactor type and target. The differences in melt production might allow to resolve the non-uniqueness of the impactor type.

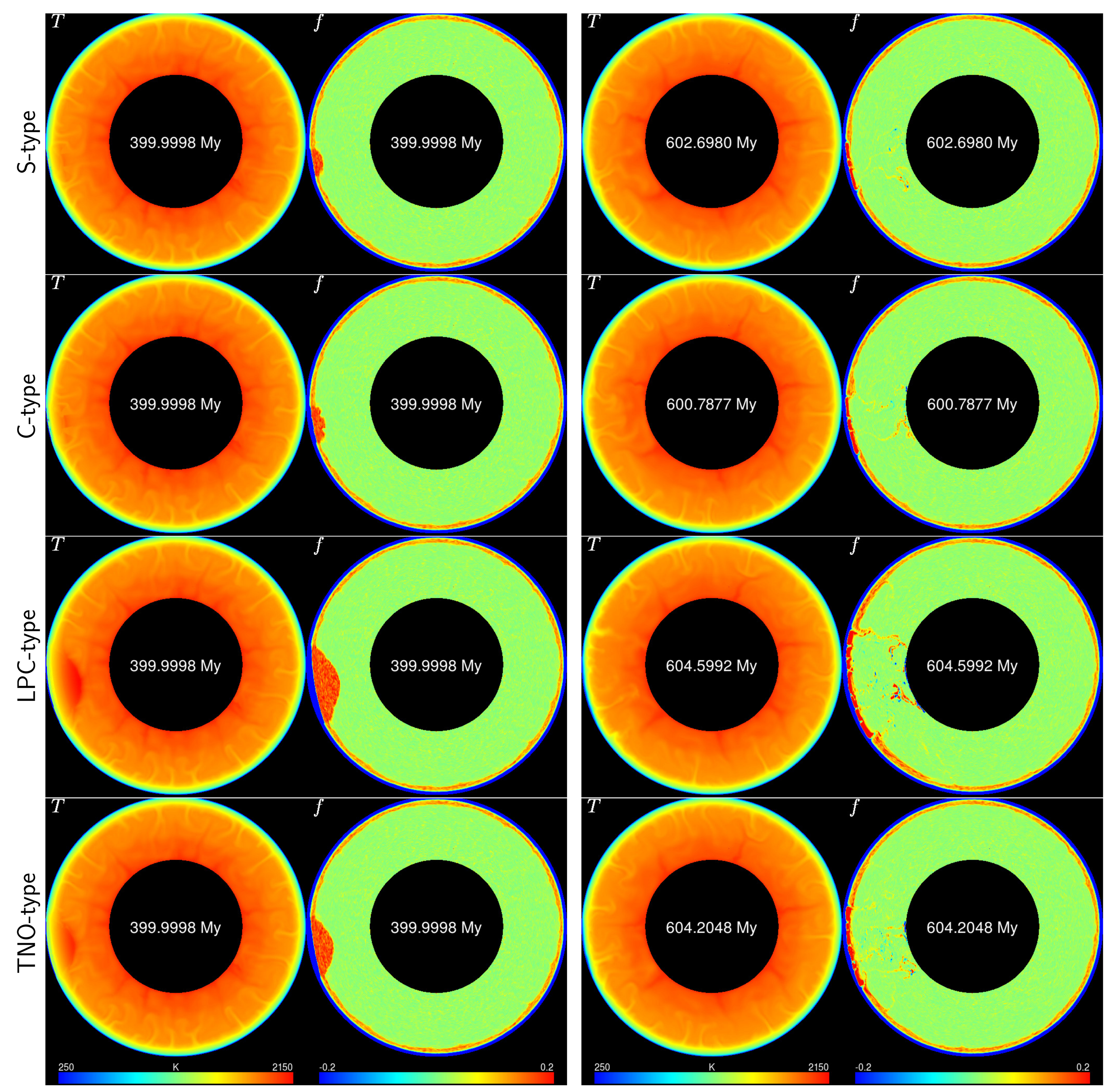

Fig. 2: Temperature (T) and depletion (f) of models with impacts on Mars by different impactor types. All four impacts occur between the 8 and the 9 o'clock position and produce a basin with the diameter of the Hematite basin (D_f = 1065 km). The left panel shows the state directly after the impact, the right panel the state 200 Myr after the impact.

Models

The Hematite basin on Mars could, in principle, have been produced by any of the four impactor types considered with the parameters given in the table below. Snapshots of the evolution are shown in Fig. 2 and show that an S- or C-type asteroid on the one hand and an LPC or TNO-type on the other hand produce similar results and would be difficult to discern on the basis of observations. The effects of the two subgroups on the interior, however, are more substantial: while the disturbances from the asteroids have largely disappeared 200 Myr later, those from the fast low-density impactors are more extensive and have a more long-lasting effect on the vigor of convection (Fig. 3) and on the large-scale flow field, as they "attract" plumes to the impact site.

Fig. 3 also shows three isocrater models for an Utopia-size event, in which the effects are larger and more diverse. Beyond a certain size, the anomalies seem to stall convection regionally for a limited time, because the affected region responds with delay.

Type	D_imp (km)	z_ic (km)	r_ic (km)	p_max (GPa)
Hematite				
S	187	52	52	42
C	255	49	70	24
LPC	159	34	161	393
TNO	169	40	132	127
Utopia				
S	700	191	193	48
C	953	181	263	26
TNO	631	149	493	134

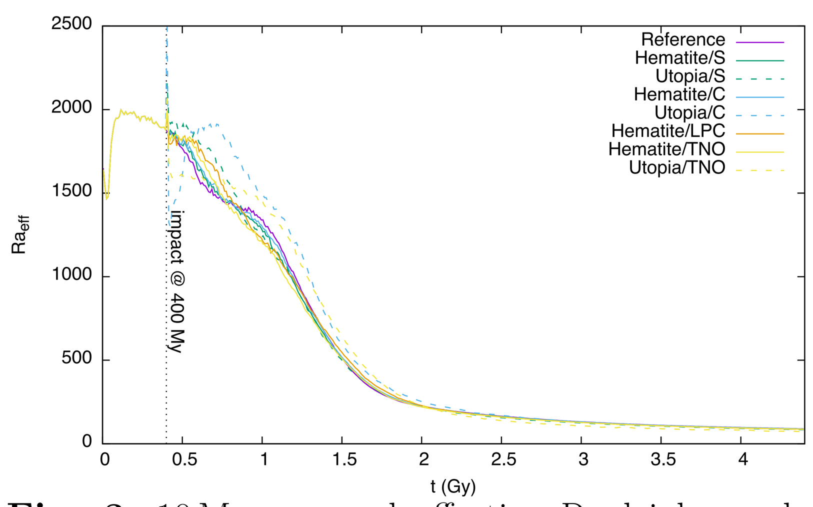

Fig. 3: 10 My-averaged effective Rayleigh number Ra/η'_ave for Hematite (solid lines) and Utopia (dashed lines) isocrater models.

Summary

Very different impactors can produce craters of the same diameter. The effects of different impactor types on the interior are partly different and may offer a means for distinguishing them. Fast low-density impactors (LPC, TNO) produce significantly larger anomalies and result in more extensive melting than asteroidal ones. The size of related observed post-impact features constrains the impactor population.

Acknowledgements

TR was supported by DFG grant Ru 1839/1-1, with additional funding from SFB-TRR 170. The models were run on the ForHLR II cluster at the Steinbuch Centre for Computing, Karlsruhe.

References

Abramov, O., S. M. Wong, D. A. Kring (2012). *Icarus, 218*, 906–916.

Bjorkman, M. D., K. A. Holsapple (1987). *Int. J. Impact Engng., 5*, 155–163.

Pierazzo, E., A. M. Vickery, H. J. Melosh (1997). *Icarus, 127*, 408–423.

Roberts, J. H., J. Arkani-Hamed (2012). *Icarus, 218*, 278–289.

Ruedas, T., P. J. Tackley, S. C. Solomon (2013). *Phys. Earth Planet. Inter., 216*, 32–58.

Tackley, P. J. (2008). *Phys. Earth Planet. Inter., 171*, 7–18.

Wänke, H., G. Dreibus (1994). *Phil. Trans. R. Soc. Lond., A 349*, 285–293.

Watters, W. A., M. T. Zuber, B. H. Hager (2009). *J. Geophys. Res., 114*, E02001.

Werner, S. C., B. A. Ivanov (2015). In: T. Spohn (ed.), *Physics of Terrestrial Planets and Moons*, volume 10 of *Treatise on Geophysics*, 2nd ed., chapter 10.10, 327–365. Elsevier.